ORIGINAL RESEARCH

Sevoflurane Alters Serum Metabolites in Elders and Aging Mice and Increases Inflammation in Hippocampus

Tingting Wang[1−3,]*, Xia Wu [4,]*, Xiaoli Zhao[2,3,]*, Jiaqi Li[5,]*, Jian Yu[4], Maozheng Sheng [4], Mingyuan Gao[4], Yutang Cao[5], Jiawen Wang[6], Xiaozhen Guo[5], Kai Zeng [1]

[1]Department of Anesthesiology, Anesthesiology Research Institute, The First Affiliated Hospital of Fujian Medical University, Fuzhou, People's Republic of China; [2]Seventh People's Hospital of Shanghai University of Traditional Chinese Medicine, Shanghai, People's Republic of China; [3]Department of Anesthesiology, Changning Maternity and Infant Health Hospital, Shanghai, People's Republic of China; [4]Shanghai Key Laboratory of Regulatory Biology, Institute of Biomedical Sciences and School of Life Sciences, East China Normal University, Shanghai, People's Republic of China; [5]State Key Laboratory of Drug Research, Shanghai Institute of Materia Medica, Chinese Academy of Sciences, Shanghai, People's Republic of China; [6]College of Life Sciences, Wuhan University, Wuhan, People's Republic of China

*These authors contributed equally to this work

Correspondence: Kai Zeng; Xiaozhen Guo, Email fymzk6822@163.com; guoxz@simm.ac.cn

Purpose: Postoperative cognitive dysfunction (POCD) is a central nervous system complication that occurs after anesthesia, particularly among the elderly. However, the neurological pathogenesis of postoperative cognitive dysfunction remains unclear. The aim of this study was to evaluate the effects of sevoflurane exposure on serum metabolites and hippocampal gene expression in elderly patients and aging mice by metabolomics and transcriptomic analysis and to explore the pathogenesis of sevoflurane induced POCD.
Patients and Methods: Human serum samples from five patients over 60 years old were collected before sevoflurane anesthesia and 1 hour after anesthesia. Besides, mice aged at 12 months (n=6 per group) were anesthetized with sevoflurane for 2 hours or with sham procedure. Subsequently, serum and hippocampal tissues were harvested for analysis. Further investigation into the relationship between isatin and neuroinflammation was conducted using BV2 microglial cells.
Results: Sevoflurane anesthesia led to the activation of inflammatory pathways, an increased presence of hippocampal astrocytes and microglia, and elevated expression of neuroinflammatory cytokines. Comparative analysis identified 12 differential metabolites that exhibited changes in both human and mouse serum post-sevoflurane anesthesia. Notably, isatin levels were significantly decreased after anesthesia. Notably, isatin levels significantly decreased after anesthesia, a factor known to stimulate proliferation and proinflammatory gene expression in microglia—the pivotal cell type in inflammatory responses.
Conclusion: Sevoflurane-induced alterations in serum metabolites in both elderly patients and aging mice, subsequently contributing to increased inflammation in the hippocampus.
Keywords: sevoflurane, hippocampus, neuroinflammation, RNA-seq, metabolomics, isatin

Introduction

Postoperative cognitive dysfunction (POCD) is a form of cognitive impairment that occurs after anesthesia during surgery.[1] Conditions such as anxiety, confusion, personality changes, and memory problems are commonly seen in elderly patients and can last for months to years.[1] Approximately 40% of patients over 60 years of age hospitalized for surgery show symptoms of POCD, and 12% of patients last for over three months.[2] These findings suggest that understanding anesthesia and perioperative care is important for elderly patients to improve their quality of life and reduce additional burden.

Sevoflurane is one of the most frequently used volatile anesthetics for rapid induction and maintenance of general anesthesia in surgical patients. However, evidence suggests that exposure of humans and animals to sevoflurane-based anesthetics, particularly with repeated exposure, can lead to neuropathological changes in the brain and long-term

1241

cognitive impairment.[3] Studies have shown that inhaled anesthetics can potentially trigger POCD.[4,5] However, the neurotoxic effects of sevoflurane remain unclear. Therefore, exploring the pathogenesis and mechanisms of POCD induced by inhalation anesthesia with sevoflurane and identifying effective targets to inhibit neurotoxicity and cognitive dysfunction are helpful in improving the postoperative patients' quality of life.

Metabolomics, focusing on the global profiling of metabolites in biofluids like serum and urine, is widely recognized as the closest reflection of the phenotype.[6,7] Metabolomics, in combination with RNA-seq to reveal key metabolites and gene alterations, provides vital information on changes in the abundance of endogenous metabolites associated with cellular responses to disease.[8] Thus, in the present study, via analyzing RNA-seq database of hippocampal tissues from sevoflurane anesthetized mice and UPLC-MS-based water-soluble metabolomics in serum samples derived from elders and aging mice anesthetized with sevoflurane, we showed that sevoflurane anesthesia induced neuroinflammation and changes in isatin levels, which might be responsible for neurocognitive deficits. Overall, our work provides novel POCD biomarkers for clinical diagnosis and potential intervention targets as well as mechanistic insights into metabolites in the hippocampus.

Materials and Methods
Study Design and Patient Population
Serum samples were collected from patients who underwent gynecological laparoscopic surgery at Changning Maternity and Infant Health Hospital, Shanghai, China. The study complies with the Declaration of Helsinki and was approved by the Ethics Committee of Changning Maternity and Infant Health Hospital, Shanghai, China (CNFBLLKT-2021-008). All study subjects signed informed written consent forms. Participants were eligible if they were aged ≥60 years and underwent minimally invasive surgery with a minimum anticipated hospital stay of two days. None of the patients received preoperative drug therapy, and blood samples were collected before and 1 h after anesthesia. The samples were stored at −80°C before use.

Animals and Sevoflurane Anesthesia
C57BL/6J mice aged at 12-month-old were purchased from the Shanghai Research Center for Model Organisms and kept in a temperature- and humidity-controlled facility at 22°C at room temperature under a 12-h light/dark cycle with free access to food. Mice were fasted for 4 hours and anesthetized with 3% sevoflurane for 2 hours. Blood was collected immediately after mice were anesthetized. Blood samples were centrifuged at 3500g for 10 min 4°C to collect serum. The serum samples were stored at −80°C before use for metabolomics. During this procedure, mice were placed in a closed chamber with a heating pad to maintain their body temperature. The control mice were placed in the same chamber without any treatment. Blood was collected immediately after mice were anesthetized. The study was approved by Ethics Committee of Animal Experiments of the East China Normal University (m20231205). All the applied procedures followed the Chinese guidelines for the welfare of the laboratory animals (GB/T 35823–2018).

RNA-Seq and Gene Enrichment Analyses
To investigate the expression profiles of genes involved in sevoflurane-induced neurotoxicity, we obtained public RNA-Seq data (GSE155770) of hippocampal tissues from postnatal day 7 (PD7) mice from the NCBI GEO (https://www.ncbi.nlm.nih.gov/geo/). FastQC (v0.11.5) was used to verify the quality of the pretreated data, which were mapped to GRCm38 using STAR (2.5.3a). The transcripts were assembled using StringTie (v1.3.1c), and the differential gene transcript expression between the control (Con) group and sevoflurane anesthesia (Sevo) group was analyzed using DESeq2 (v1.16.1). The differential threshold value was p-value <0.05, and fold change >1. All analyses described above were performed using R version 4.2.2.

Untargeted Metabolomics Analysis Using UPLC-Q/TOF-MS
Serum samples were obtained from patients both pre-anesthesia and one-hour post-sevoflurane anesthesia, as well as mouse serum samples from the control group and the sevoflurane-treated group. Sample preparation was performed as described previously.[9,10]

Non-targeted metabolomics were performed using an ultrahigh-performance liquid chromatography system (UPLC; Waters, Milford, MA, USA) equipped with a quadrupole time-of-flight mass spectrometer (Q/TOF; Waters). Plasma metabolites were

separated on an Acquity UPLC BEH C18 (2.1 × 50 mm, 1.7 μm, Waters) at an optimized column temperature of 40 °C with an injection volume of 5 μL. Gradient elution was performed using 0.1% aqueous formic acid (A) and acetonitrile: isopropanol (B, 90:10, v/v) at a flowrate of 0.4 mL/min. For the mass spectrum analysis, the acquisition mode was a full scan with fragmentation under positive and negative polarity. The Q/TOF mass analyzer was operated at 22,000 mass resolution, and scan range of m/z 50–1500 Da. The comprehensive workflow for the untargeted metabolomic analysis included retention time correction, experimental design setup, peak picking, normalization, deconvolution, and alignment in QI (version 3.0, Waters Corp., Milford, MA, USA). The differential metabolites were further imported into MetaboAnalyst (version 5.0) to conduct a Kyoto Encyclopedia of Genes and Genomes (KEGG) pathway enrichment analysis. Heatmaps and Venn diagrams were obtained from Hiplot (Shanghai, China). Subsequently, multi-omics analysis was performed utilizing the Joint Pathway Analysis (JPA) module from MetaboAnalyst 5.0 that enables the combination of transcriptomics and metabolomics data for functional enrichment analysis and pathway topology analysis.[11]

Immunohistochemistry

Mice were deeply anesthetized and perfused with 4% paraformaldehyde. Brain samples were dehydrated with 30% sucrose overnight and sectioned into 40-μm coronal slices using a Leica CM1950 cryostat. The brain slices were rinsed twice in phosphate-buffered saline (PBS), blocked with goat serum at room temperature for 1 h, and incubated at 4°C overnight with the following primary antibodies: rabbit anti-GFAP (BOSTER, BA0056, 1:500) and goat anti-IBA1 (Abcam, ab5076, 1:500). Brain slices were washed three times in PBS and incubated for 2 h with the following secondary antibodies: anti-rabbit-Alexa Fluor 488 or anti-goat-Alexa Fluor 488. After washing, the sections were mounted using the Hoechst solution. Images were captured using a Leica confocal microscope and analyzed using the ImageJ software.

Inflammatory Gene Expression Assay

Experimental mice were exposed to or without sevoflurane for 2 h. The mice were sacrificed, and the hippocampus was quickly removed and frozen in liquid nitrogen. Total RNA was isolated from the hippocampal tissue using RNAiso Plus (Takara, 9108) following the manufacturer's instructions. The RNA concentration was determined using a NanoDrop Microvolume Spectrophotometer and Fluorometer (Thermo Fisher Scientific). For qPCR analysis, 1 μg of total RNA was reverse-transcribed into cDNA using the PrimeScriptTMRT Master Mix (Takara, RR036A). qPCR analysis was performed using a quantitative real-time PCR system (Roche, LightCycler 480) with SYBR Green Master Mix (Thermo Fisher Scientific, 4309155). An internal control using the GAPDH gene for data analysis and cycle threshold (Ct) values were calculated using the $2^{-\Delta\Delta Ct}$ method.

Primers:

Il-1β-F TGGACCTTCCAGGATGAGGACA
Il-1β-R GTTCATCTCGGAGCCTGTAGTG
Il-6-F TACCACTTCACAAGTCGGAGGC
Il-6-R CTGCAAGTGCATCATCGTTGTTC
Il-8-F GGTGATATTCGAGACCATTTACTG
Il-8-R GCCAACAGTAGCCTTCACCCAT
Tnf-α-F GGTGCCTATGTCTCAGCCTCTT
Tnf-α-R GCCATAGAACTGATGAGAGGGAG
Ccl2-F GCTACAAGAGGATCACCAGCAG
Ccl2-R GTCTGGACCCATTCCTTCTTGG
CyclinA1-F GCTACTGAGGATGGAGCATCTG
CyclinA1-R CAGCTTCCAGAAGGCTCAGTTC
CyclinB1-F AAGGTGCCTGTGTGTGAACC
CyclinB1-R GTCAGCCCCATCATCTGCG
CyclinE1-F GTGGCTCCGACCTTTCAGTC
CyclinE1-R CACAGTCTTGTCAATCTTGGCA

Cell Viability Assay

The BV2 microglial cell line was purchased from the National Infrastructure of Cell Line Resource (China). BV2 microglial cells were seeded in 96-well plates (1×10^4 cells/well) and treated with 100 ng/mL LPS for 2 h, followed by incubation with isatin (Aladdin, 5–25 μM) for 24 h. Cells were treated with different concentrations of isatin and assessed by a tetrazolium salt reduction assay using a cell counting kit-8 (CCK8) assay. After 24 h of treatment with or without isatin, CCK8 solution was added to each well in 96-well plates of different groups and incubated at 37°C for 2 h prior to measuring the absorbance value at 450 nm using a microplate reader (BioTek Synergy Neo2).

Cell Proliferation Analysis

The EdU Cell Proliferation Assay Kit (Beyotime, China) was used to measure the cell proliferation. BV2 microglia cultured with or without 25μM isatin were incubated in fresh medium containing 50 μM 5-ethynyl-20-deoxyuridine (EdU) at 37°C for 2 h. After rinsing with PBS, cells were fixed in 4% paraformaldehyde for 15 min and treated with 0.5% Triton X-100 for 10 min. Hoechst 3342 was used to stain the nuclei for 10 min. Finally, the number of EdU-positive BV2 cells was counted.

Statistical Analysis

All data are presented as mean ± SEM. Data analysis was performed using GraphPad Prism 9. Data normality test was performed using the Shapiro–Wilk normality test. A two-tailed t-test was performed to identify the differences between the two groups. One-way ANOVA was used to test the homogeneity of variance between groups. p-value <0.05.

Results

Sevoflurane Induced Inflammatory Gene Programs in Hippocampus

To investigate the differential gene expression profiles caused by sevoflurane treatment, we analyzed public RNA-Seq data of the mouse hippocampus (GSE155770). The PCA score plot revealed a distinct separation between the expression profiles of sevoflurane and control groups (Figure 1A). The volcano plot and heatmap revealed 207 upregulated and 117 downregulated mRNAs (fold change>2, $p < 0.05$; heatmap only showed the top 50 genes) among the 18,855 detected mRNAs following sevoflurane exposure in mice (Figure 1B and C, Supplementary Table 1). Notably, the expressions of *Nppb* (natriuretic peptide type B) and *Itk* (T cell kinase) were among the top increased genes in the hippocampus of sevoflurane treated mice, which have been previously suggested to be involved in nervous system activities and disorders.[12–14] Itk signaling is critical for regulating the differentiation and function of CD4+ T cells and facilitating CD4+ T cell migration to the central nervous system to promote neuroinflammation.[14] Meanwhile, it has been reported that lesional and non-lesional IL-31 transgenic mice also exhibit increased *Nppb* transcripts in the DRGs and skin.[12] These results suggest that sevoflurane exposure promotes neuroinflammation.

KEGG pathway analysis uncovered notable enrichment in starch and sucrose metabolism, carbohydrate digestion and absorption, IL-17 signaling pathway, TNF-α signaling pathway, and chemokine signaling pathway following sevoflurane treatment (Figure 1D), which is consistent with previous reports showing the secretion of inflammatory and oxidative stress mediators are associated with neurological diseases such as multiple sclerosis (MS),[15] chronic itch[16] and experimental autoimmune encephalomyelitis (EAE).[17,18] Microglial activation-mediated neuroinflammation plays an important role in neurodegenerative disease progression. Glycolysis is involved in microglial activation and inhibition of glycolysis ameliorates microglial activation-related neuroinflammatory diseases.[19] In addition, renin secretion, Wnt signaling pathway, sphingolipid signaling pathway, and cAMP signaling pathway were reduced in the sevoflurane group compared with the control group (Figure 1E), suggesting a decline in neuron functionality.

Gene Ontology Analysis Explored the Regulatory Mechanism of Sevoflurane Induced Inflammation in Hippocampus

The major Gene Ontology (GO) functional terms of the differential expression genes (DEGs), including biological process (BP), molecular function (MF), and cellular component (CC) ontologies, are illustrated in Figure 2. The GO enrichment analysis of
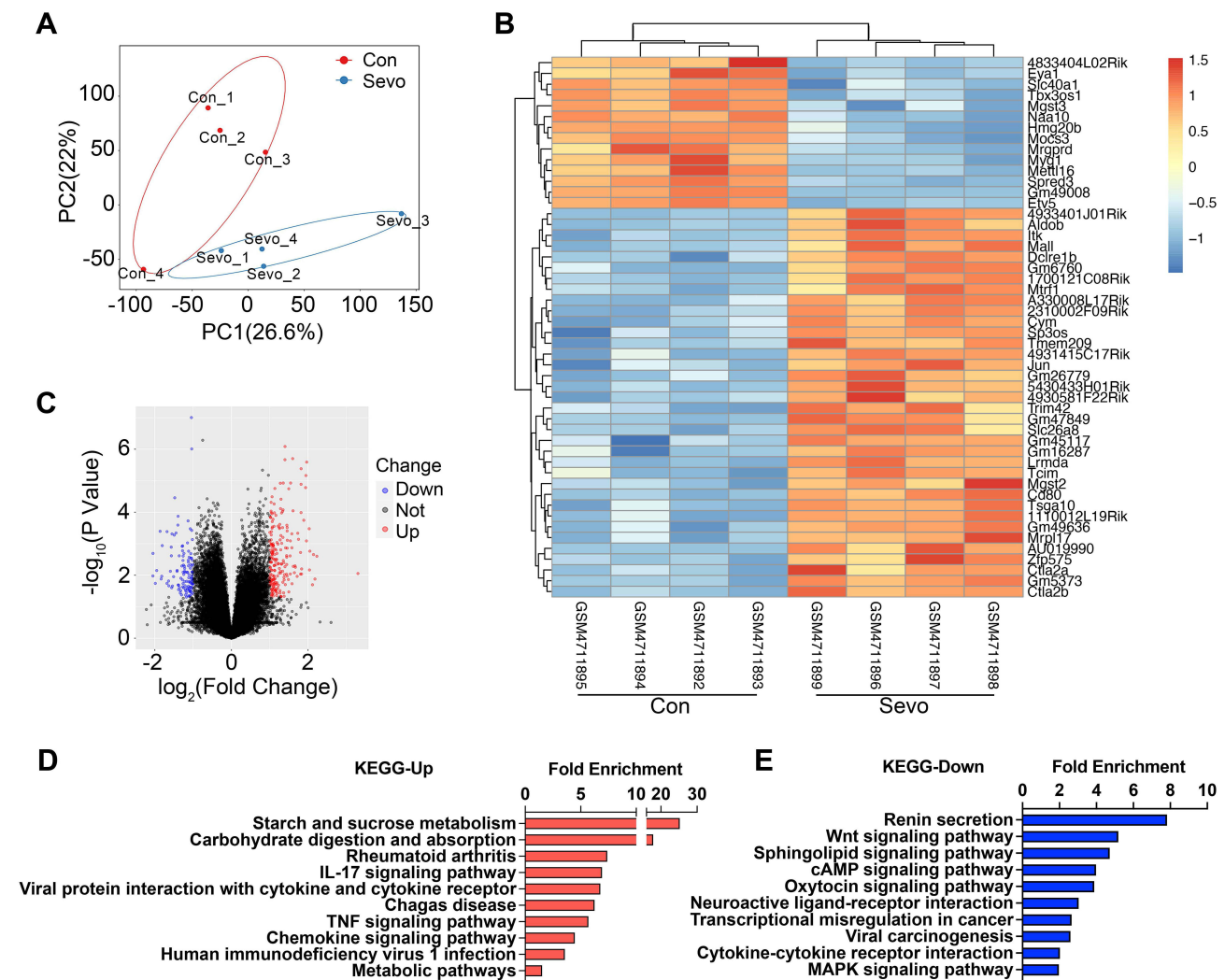
Figure 1 Transcriptome analysis of hippocampal tissues in the sevoflurane anesthetized (Sevo) vs control groups (Con) of mice.
Notes: (**A**) PCA score plot revealed a distinct separation between expression profiles in sevoflurane and control groups. (**B**) Top 50 altered genes in heatmap from hippocampal tissues in the Sevo group compared with the Con group. (**C**) Volcano plot showing differentially expressed genes (up- and downregulated) from hippocampal tissues in the Sevo group compared with the Con group. The red dots represent the upregulated genes, and the blue dots represent the downregulated genes. (**D**) KEGG analysis assessing the pathways associated with the upregulated gene sets. (**E**) KEGG analysis assessing the pathways associated with the downregulated gene sets.

biological processes suggested that the meiotic cell cycle process and positive regulation of the DNA binding process were upregulated (Figure 2A), while cellular metal ion homeostasis, cellular cation homeostasis, and divalent metal ion transport were downregulated (Figure 2B), indicating multiple-disease conditions, such as ischemic brain injury, multiple sclerosis, Alzheimer's disease, and drug addiction.[20] Indeed, the disruption of intracellular ion homeostasis is common mechanism of oxidative stress damage induced cell death.[21] GO-MF and GO-CC analyses indicated that the DEGs were significantly enriched with respect to ion channels and transmembrane transporters (Figure 2C and E). In addition, transcription and secretory vesicles were reduced (Figure 2D and F), suggesting that anesthesia might induce disruption of *de novo* gene transcription and synthesis of proteins involved in neural plasticity. This is in consistent with previous findings that prolonged exposure to sevoflurane leads to cognitive deficiency and disproportion of excitatory/inhibitory synapses during brain development.[22,23]

Sevoflurane Induced Neuroinflammatory Activation in Hippocampus

Considering that inflammatory and oxidative responses were increased in sevoflurane-treated mice in RNA-seq analysis, we next investigated *Iba1*^{+} microglia and GFAP-enriched astrocytes by immunofluorescence, which are closely linked to brain injury and inflammatory responses.[24] After 2 hours of sevoflurane exposure, the fluorescence intensity of GFAP in the hippocampus
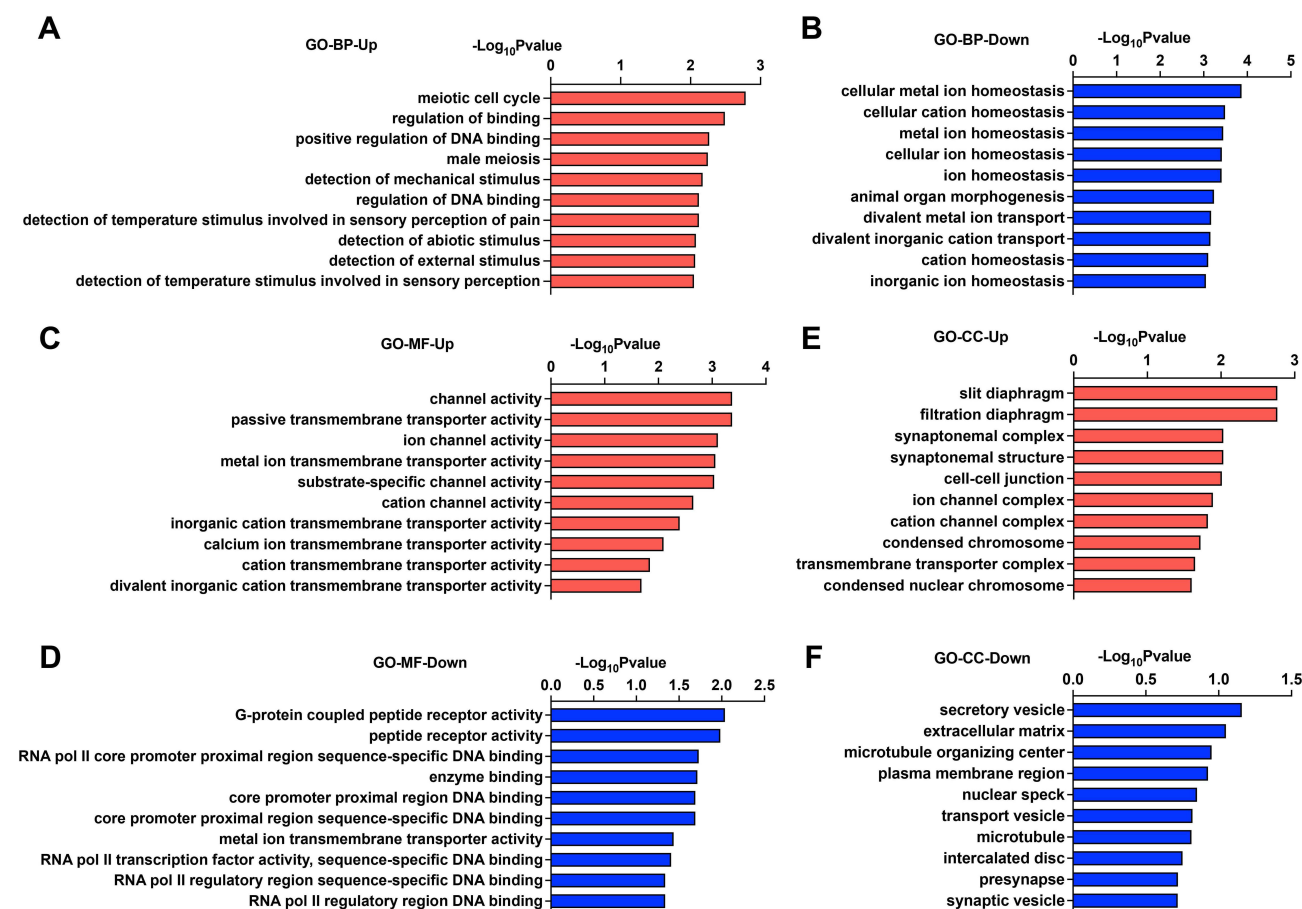
Figure 2 GO analysis of hippocampal tissues in the Sevo group compared with the Con group.
Notes: (**A** and **B**) GO analysis of the biological process of upregulated (**A**) and downregulated (**B**) differential genes. (**C** and **D**) GO analysis of the molecular function of upregulated (**C**) and downregulated (**D**) differential genes. (**E** and **F**) GO analysis of the cell component of upregulated (**E**) and downregulated (**F**) differential genes.

significantly increased (Figure 3A–C), suggesting a strong effect of sevoflurane exposure on promoting astrocyte accumulation in the hippocampus. We also found that the percentage of *Iba1*+ microglia was significantly higher in the hippocampus (Figure 3D–F) after 2 hours of sevoflurane exposure compared to control mice. Transcription analysis of inflammatory genes in the hippocampi of mice showed that the expression of *Il-1β, Il-6, Il-8* and *Tnf-α* was significantly augmented after sevoflurane exposure (Figure 3G–J), suggesting that postoperative sevoflurane anesthesia induced inflammatory gene expression in the hippocampal tissue.

Significant Metabolic Change Induced by Sevoflurane Anesthesia in Human and Mouse Serum

Serum metabolites represent systematic alterations in metabolism. RNA-seq analysis suggested that metabolism was altered in the hippocampus of mice treated with sevoflurane. Thus, we further examined metabolites using metabolomics in the serum of both mice and humans before and after sevoflurane anesthesia. In the mouse serum, 341 metabolites were differentially expressed between the control and sevoflurane groups. Among them, a total of 82 metabolites were increased and 259 metabolites were decreased in sevoflurane treated group (Figure 4A). The top 10 upregulated or downregulated pathways with the highest enrichment ratios are shown in Figure 4B. The top upregulated pathways included steroid hormone biosynthesis, butanoate metabolism, and tryptophan metabolism, whereas the downregulated pathways included arginine and proline metabolism, aminoacyl-tRNA biosynthesis, and tryptophan metabolism.

Notably, for clinical purposes, we collected human serum from patients aged over 60-year-old under surgery before and immediately after sevoflurane anesthesia. In total, 114 metabolites were differentially expressed. Compared with pre-
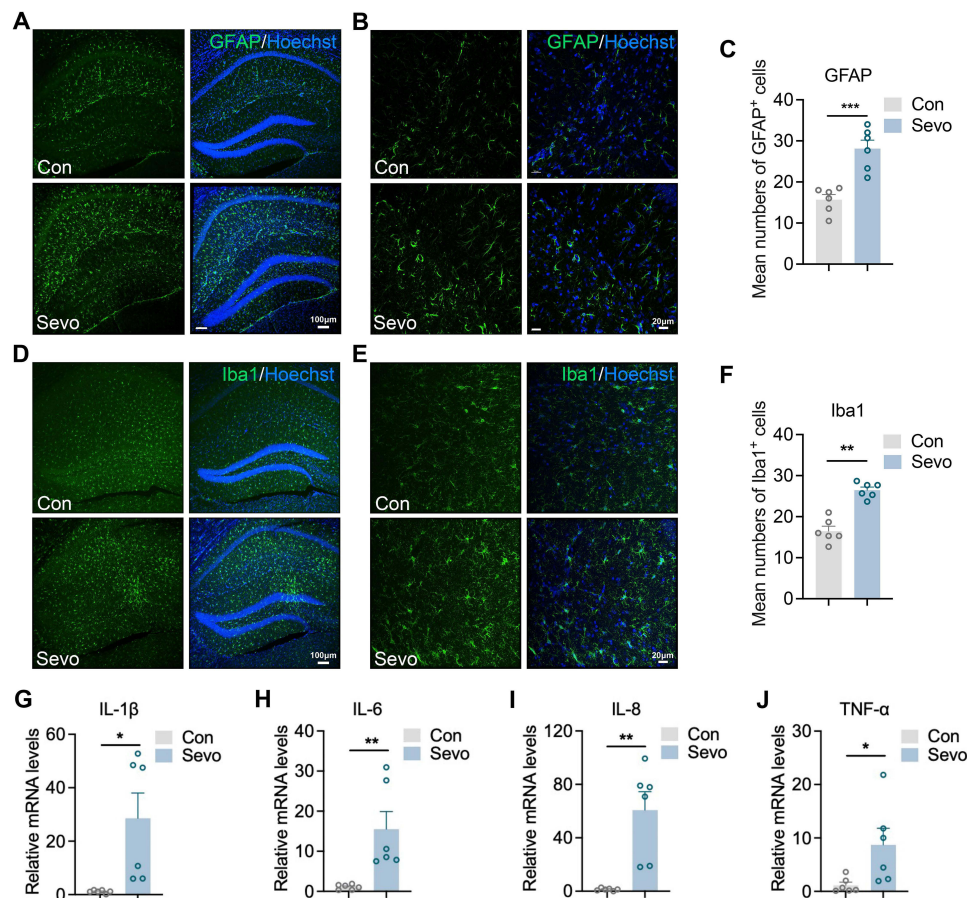
Figure 3 Sevoflurane anesthesia induce neuroinflammation of hippocampus.
Notes: (**A-F**) Hippocampal sections of the mice were immunostained for GFAP (**A** and **B**) and IBA1 (**D–E**). Immunofluorescence detection of the astrocytic marker GFAP protein and of the microglial marker IBA1 in the rat hippocampus (40μm) from mice sevoflurane either anesthesia or not for 2 hours. (**C, F**) The image is displayed at 200x the original magnification and was used for the quantification of hippocampal astrocyte and microglia numbers. The mean numbers of hippocampal astrocytes and microglia were quantified in the regions displayed on the right. (**G-J**) Time course of the induction of mRNA expression of inflammatory mediators, including *Il6, Il8, Il1β* and *Tnfα* in the hippocampi of from mice sevoflurane either anesthesia or not for 2 hours. All mRNA species were quantified relative to the expression of the housekeeping gene *GAPDH* and are presented as fold changes relative to controls. All displayed values are reported as the mean ± SEM. *p < 0.05; **p < 0.01; ***p < 0.001 vs control group. n=6 per group.

anesthesia, a total of 58 metabolites were significantly increased, while 56 metabolites were decreased after anesthesia (Figure 4C). KEGG pathway enrichment analysis revealed that the upregulated differentially expressed metabolites were enriched for nicotinate and nicotinamide metabolism, porphyrin and chlorophyll metabolism, and arginine biosynthesis. The downregulated differential metabolites were enriched in multiple amino acid and nucleotide metabolism pathways, including pyrimidine metabolism; glycine, serine, and threonine metabolism; and cysteine and methionine metabolism (Figure 4D).

Comparison of Metabolic Change Identified in Human and Mouse Serum

To further understand the key metabolic pathways and metabolites caused by sevoflurane anesthesia, we constructed a Venn diagram and found that four KEGG pathways were consistently altered in human and mouse serum, including tyrosine metabolism, glycine, serine, and threonine metabolism, cysteine and methionine metabolism, and tryptophan metabolism (Figure 5A and B). We further performed multi-omics analysis using the Joint Pathway Analysis (JPA) module from MetaboAnalyst 5.0, which can combine transcriptomic and metabolomics data for functional enrichment analysis and pathway topology analysis.[11] According to combined enrichment and network topology metrics, the top metabolic pathways were Cysteine and methionine metabolism and Tyrosine metabolism (Figure 5C), which were consistent with overlapping KEGG pathways in human and mouse serum (Figure 5B). In addition, detailed analysis of
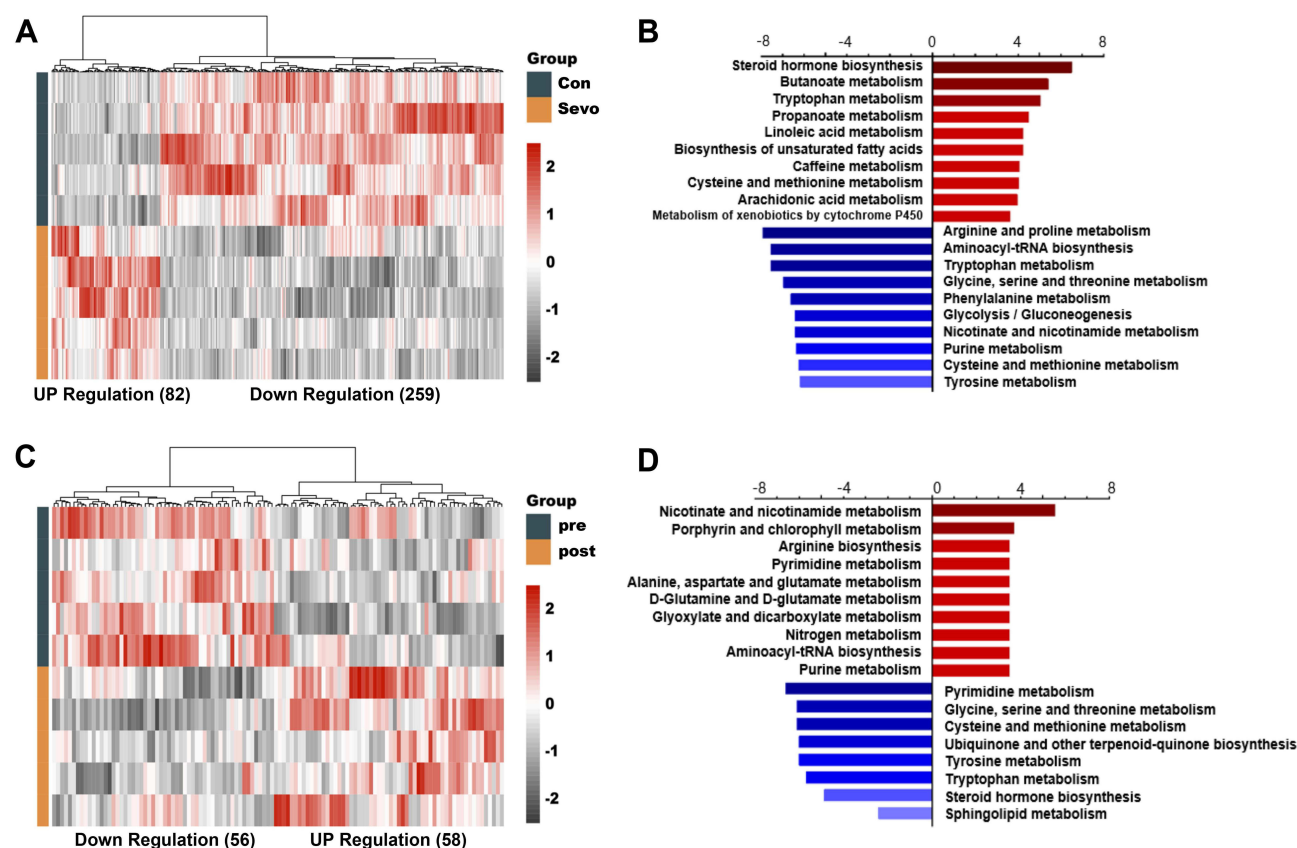
Figure 4 Differential metabolites before and after sevoflurane treatment.

Notes: (**A**) Heatmaps of pre- and post-anesthesia differential metabolites in mouse serum. (**B**) Kyoto Encyclopedia of Genes and Genomes pathway enrichment analysis for differential metabolites in mouse serum. (**C**) Heatmaps of control and anesthesia differential metabolites in human serum. (**D**) Kyoto Encyclopedia of Genes and Genomes pathway enrichment analysis for differential metabolites in human serum.

the metabolites revealed that hydroxystearic acid was significantly increased and maleylacetoacetic acid, isatin, cysteine-S-sulfate, and 3-O-methyldopa were significantly decreased after anesthesia (Figure 5D–F).

Isatin Inhibits Neuroinflammation and Microglia Proliferation

Of note, we noticed that a downregulated metabolite, isatin, which was substantially consistent with the secondary fragments of the standard substance (Supplementary Figure 1), exhibited neuroprotective effects in different experimental models of neurodegeneration by enhancing cellular antioxidant, anti-inflammatory, and detoxification mechanisms.[25,26]

Thus, we explored whether isatin influences the biological function of microglial cells, considering that microglia are resident macrophages in the brain and sensitive to pathogens or damages by promoting the secretion of molecular signals to trigger reactive astrocytes.[27] To determine the potential cytotoxicity of isatin, we analyzed its dose-dependent effects on the survival of BV2 microglial cells. The results demonstrated that isatin was not cytotoxic to BV2 microglial cells at the tested concentrations (Figure 6A). To further explore the effects of isatin on microglia, we cultured BV2 microglial cells in the presence of LPS, the most widely used inflammatory model, with or without isatin. Our data showed that isatin significantly suppressed mRNA expression of *Tnf-α, Il-1β, Il-6*, and *Ccl2* in LPS-stimulated BV2 cells (Figure 6B–E).

In addition, as shown in Figure 3F, we found that microglial numbers were significantly increased in the hippocampus after sevoflurane exposure. Consequently, we investigated whether isatin inhibits microglial proliferation. Indeed, the expression of cyclins A1, B1, and E1 in the isatin group was significantly suppressed compared with that in the control group (Figure 6F). EdU staining also indicated that isatin inhibited BV2 microglial proliferation (Figure 6G and H).
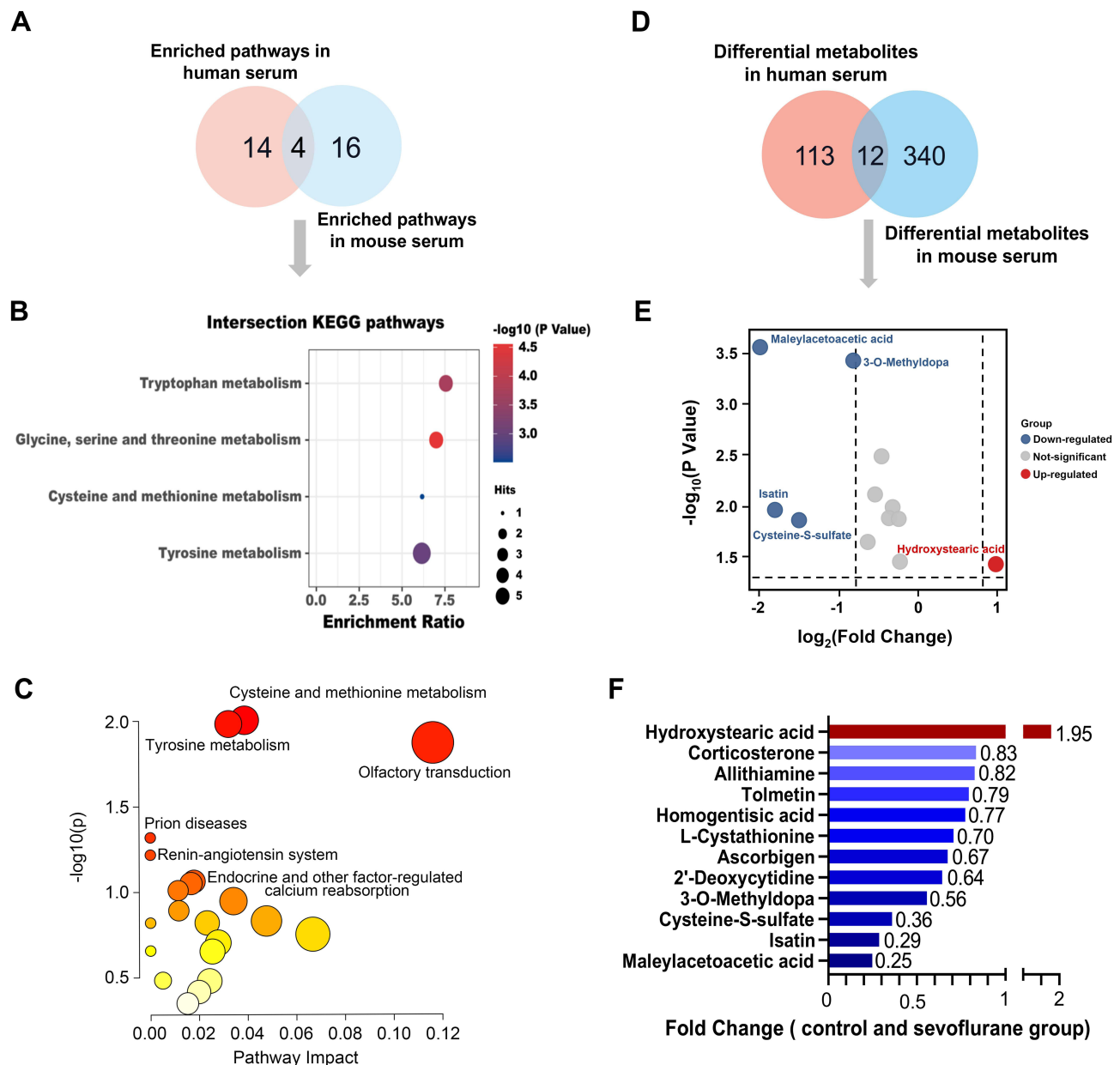
A

Enriched pathways in
human serum

Enriched pathways
in mouse serum

B

C

D

Differential metabolites
in human serum

Differential metabolites
in mouse serum

E

F

Figure 5 The overlaps of differential metabolites between mouse and human serum.
Notes: (**A**) Venn diagram depicting Intersection KEGG pathways. (**B**) Kyoto Encyclopedia of Genes and Genomes analysis assessing the overlapping pathways between human and mouse serum. (**C**) JPA module conducts multi-omics analysis on transcriptomic and metabolomic data. Y-axis, enrichment significance; X-axis, pathway impact for network topology. (**D**) Venn diagram depicting the number of unique and overlapping metabolites. (**E**) Volcano plot showing different metabolites (up- and downregulated) from hippocampal tissues in the Sevo group compared with the Con group. The red dots represent the upregulated metabolites, and the blue dots represent the downregulated metabolites. (**F**) Diagrams depict the fold change of overlapping metabolites.

These data suggested that isatin suppressed the proliferation and inflammatory properties of microglial cells. The reduction in isatin levels after sevoflurane anesthesia may lead to neuroinflammation in the hippocampus.

Discussion

POCD is a central nervous system complication that occurs after anesthesia. Neuroinflammation caused by general anesthesia is an important factor in the pathogenesis of POCD.[28] The exacerbation of neuroinflammation produces deleterious outcomes, such as delirium and accelerated disease progression, merits careful investigation in humans. Sevoflurane, a commonly used alkane inhalation anesthetic, induces hippocampal neuronal inflammation and apoptosis in
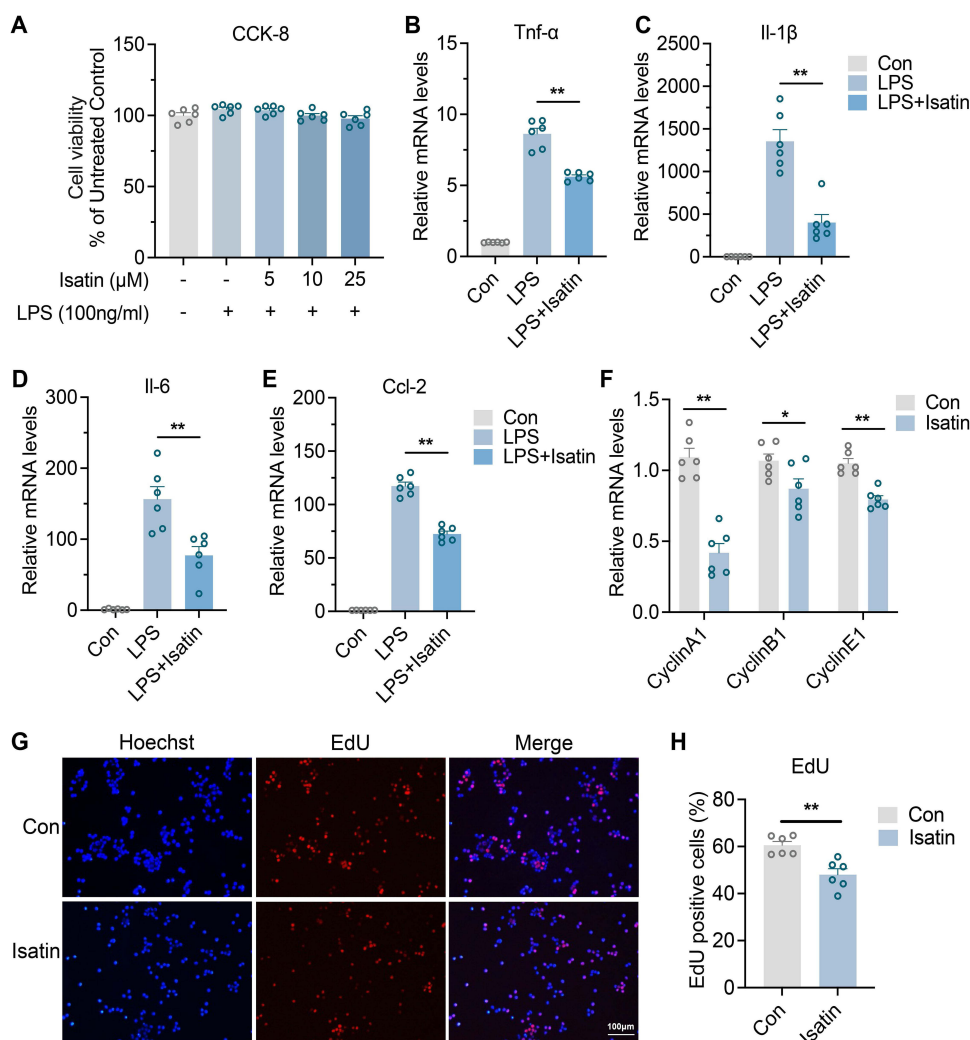
Figure 6 Isatin inhibits neuroinflammation and microglia proliferation.
Notes: (**A**) Statistical histograms showed the BV2 cell viability after treatment with 100ng/mL LPS and different concentrations of isatin. mRNA levels of inflammatory factors *Tnf-α* (**B**), *Il-1β* (**C**), *Il-6* (**D**), and *Ccl2* (**E**) and proliferative factors (**F**) in BV2 cell treated either vehicle or isatin (25 μM) (**G**) Representative EdU staining image of BV2 cells 24 h after vehicle or isatin treatment. (**H**) Histogram indicating the number of proliferating cells in the control or isatin groups. Data was shown as mean ± SEM. *$p < 0.05$; **$p < 0.01$ vs control group. n=6 per group.

older rats, leading to cognitive dysfunction.[29] However, the underlying mechanisms remain unclear. In the present study, we found that sevoflurane caused changes in serum metabolites in both aged humans and mice, potentially leading to increased microglia and astrocytes, as well as acute inflammation in the hippocampus.

Neuroinflammation is vital for pathological dysfunction of the neuronal system. The interplay between microglia and astrocytes significantly influences neuroinflammation. It has been previously shown that neuroinflammation and ischemia induced microglia activation and then reactive astrocytes in central nervous system (CNS).[27,30] Microglial cells are resident immune effector cells of the CNS and play critical roles for inflammation-associated neurotoxicity.[31] Here, we identified that astrocytes and microglia were significantly increased, accompanied with high expressions of pro-inflammatory factors after sevoflurane exposure, suggesting that sevoflurane anesthesia induces hippocampal neuroinflammation. Interestingly, KEGG pathway analysis enriched not only inflammatory pathways but also starch and sucrose metabolism pathways, emphasizing the role of glucose metabolism in regulating brain injury after sevoflurane exposure. Glucose metabolism is actively implicated in microglia activation-mediated inflammatory responses, consistent with previous reports that inflammatory activation of microglial cells and astrocytes is often accompanied by a metabolic switch from oxidative phosphorylation to aerobic glycolysis.[19,32] Recruitment and activation of astrocytes and microglia

require the complex spatio-temporal communication between neurons and glia, as well as between glial cells. How glia participate in phenotypic switches and influence surrounding glial cells and neurons requires further investigation.

Next, we investigated changes in serum metabolites before and after sevoflurane anesthesia, which indicate health status or chronic disease risk in the subjects. We found that hydroxystearic acid significantly increased, while maleylacetoacetic acid, isatin, cysteine-S-sulfate, and 3-O-methyldopa (3-OMD) significantly decreased after anesthesia. Hydroxystearic acid has anti-inflammatory effects in mice with high-fat diet-induced diabetes,[33] and maleylacetoacetic acid is the main cause of liver and kidney damage,[34] both of which may have compensatory effects following sevoflurane anesthesia. In addition, 3-OMD is a key screening biomarker for Aromatic L-amino acid decarboxylase (AADC) deficiency,[35] which is a major metabolite of L-DOP1A. 3-OMD inhibited dopamine transporter and uptake in rat brain striatal membranes and PC12 cells, and 3-OMD induced cytotoxic effects via oxidative stress and decreased mitochondrial membrane potential in PC12 cells, indicating that 3-OMD has the potential to cause damage to neuronal cells.[36,37] Subsequently, we focused on the effect of isatin, a compound known for its neuroprotective properties, which was significantly decreased in serum samples after sevoflurane anesthesia.

Isatin (indole-2,3-dione) is ubiquitously present, and its derivatives readily cross the blood–brain barrier.[38] Isatin is an endogenous indole found in both the mammalian brain and peripheral tissues, with elevated levels observed under stress conditions. It is anxiogenic at lower doses, and sedatives at higher doses.[39] It is well known for its diverse biological activities, including antitumor, antibacterial, antifungal, antiparasitic, antiviral, antioxidant and anti-inflammatory properties,[40] our study revealed that isatin treatment suppressed the expression of proinflammatory factors in microglia following LPS induction. We speculate that isatin may affect the phenotypic transformation of microglia. Interestingly, we found that isatin inhibits microglial proliferation, indicating that isatin may affect physiological glial cell function by altering the hippocampal inflammatory environment. The potential impact of isatin on POCD demands future investigation. In conclusion, our study showed that sevoflurane anesthesia affected peripheral serum metabolomic profiles, contributing to neuroinflammation. These findings may provide more insightful clues on anesthesia-induced POCD.

Ethics Statement

The study complies with the Declaration of Helsinki and was approved by the Ethics Committee of Changning Maternity and Infant Health Hospital, Shanghai, China (CNFBLLKT-2021-008). All study subjects signed informed written consent forms. The ethics of the animal experimental protocol was approved by Ethics Committee of Animal Experiments of the East China Normal University (m20231205). All the applied procedures followed the Chinese guidelines for the welfare of the laboratory animals (GB/T 35823-2018).

Author Contributions

All authors made a significant contribution to the work reported, whether in the conception, study design, execution, acquisition of data, analysis, and interpretation, or in all these areas, took part in drafting, revising, or critically reviewing the article; gave final approval of the version to be published; have agreed on the journal to which the article has been submitted; and agree to be accountable for all aspects of the work. All the authors have read and approved the final manuscript.

Funding

Disclosure

The authors report no conflicts of interest in this work.

References

1. Needham MJ, Webb CE, Bryden DC. Postoperative cognitive dysfunction and dementia: what we need to know and do. *Br J Anaesth*. 2017;119 (suppl_1):i115–i125. doi:10.1093/bja/aex354

2. Rundshagen I. Postoperative cognitive dysfunction. *Dtsch Arztebl Int*. 2014;111(8):119–125. doi:10.3238/arztebl.2014.0119

3. Tang X, Zhao Y, Zhou Z, et al. Resveratrol mitigates sevoflurane-induced neurotoxicity by the SIRT1-dependent regulation of BDNF expression in developing mice. *Oxid Med Cell Longev*. 2020;2020:9018624. doi:10.1155/2020/9018624

4. Zhou Y, Zhang Y, Wang H, Zhang X, Chen Y, Chen G. Microglial pyroptosis in hippocampus mediates sevolfurane-induced cognitive impairment in aged mice via ROS-NLRP3 inflammasome pathway. *Int Immunopharmacol*. 2023;116:109725. doi:10.1016/j.intimp.2023.109725

5. Eckenhoff RG, Johansson JS, Wei H, et al. Inhaled anesthetic enhancement of amyloid-beta oligomerization and cytotoxicity. *Anesthesiology*. 2004;101(3):703–709. doi:10.1097/00000542-200409000-00019

6. Rutledge J, Oh H, Wyss-Coray T. Measuring biological age using omics data. *Nat Rev Genet*. 2022;23(12):715–727. doi:10.1038/s41576-022-00511-7

7. Wang R, Li B, Lam SM, Shui G. Integration of lipidomics and metabolomics for in-depth understanding of cellular mechanism and disease progression. *J Genet Genomics*. 2020;47(2):69–83. doi:10.1016/j.jgg.2019.11.009

8. Nielsen J. Systems biology of metabolism. *Annu Rev Biochem*. 2017;86(1):245–275. doi:10.1146/annurev-biochem-061516-044757

9. Xu H, Wang J, Liu Y, et al. Development of a simultaneous quantification method for the gut microbiota-derived core nutrient metabolome in mice and its application in studying host-microbiota interaction. *Anal Chim Acta*. 2023;1251:341039. doi:10.1016/j.aca.2023.341039

10. Xie G, Wang L, Chen T, et al. A metabolite array technology for precision medicine. *Anal Chem*. 2021;93(14):5709–5717. doi:10.1021/acs.analchem.0c04686

11. Pang Z, Zhou G, Ewald J, et al. Using MetaboAnalyst 5.0 for LC-HRMS spectra processing, multi-omics integration and covariate adjustment of global metabolomics data. *Nat Protoc*. 2022;17(8):1735–1761. doi:10.1038/s41596-022-00710-w

12. Meng J, Moriyama M, Feld M, et al. New mechanism underlying IL-31-induced atopic dermatitis. *J Allergy Clin Immunol*. 2018;141(5):1677–1689 e8. doi:10.1016/j.jaci.2017.12.1002

13. Algahtani MM, Alshehri S, Alqarni SS, et al. Inhibition of ITK signaling causes amelioration in sepsis-associated neuroinflammation and depression-like state in mice. *Int J Mol Sci*. 2023;24(9):8101. doi:10.3390/ijms24098101

14. Kannan AK, Kim DG, August A, Bynoe MS. Itk signals promote neuroinflammation by regulating CD4+ T-cell activation and trafficking. *J Neurosci*. 2015;35(1):221–233. doi:10.1523/JNEUROSCI.1957-14.2015

15. Miller ED, Dziedzic A, Saluk-Bijak J, Bijak M. A review of various antioxidant compounds and their potential utility as complementary therapy in multiple sclerosis. *Nutrients*. 2019;11(7):1528. doi:10.3390/nu11071528

16. Wang ZH, Feng Y, Hu Q, et al. Keratinocyte TLR2 and TLR7 contribute to chronic itch through pruritic cytokines and chemokines in mice. *J Cell Physiol*. 2023;238(1):257–273. doi:10.1002/jcp.30923

17. Di Prisco S, Merega E, Lanfranco M, Casazza S, Uccelli A, Pittaluga A. Acute desipramine restores presynaptic cortical defects in murine experimental autoimmune encephalomyelitis by suppressing central CCL5 overproduction. *Br J Pharmacol*. 2014;171(9):2457–2467. doi:10.1111/bph.12631

18. Wang X, Deckert M, Xuan NT, et al. Astrocytic A20 ameliorates experimental autoimmune encephalomyelitis by inhibiting NF-kappaB- and STAT1-dependent chemokine production in astrocytes. *Acta Neuropathol*. 2013;126(5):711–724. doi:10.1007/s00401-013-1183-9

19. Cheng J, Zhang R, Xu Z, et al. Early glycolytic reprogramming controls microglial inflammatory activation. *J Neuroinflammation*. 2021;18(1):129. doi:10.1186/s12974-021-02187-y

20. Ruan N, Tribble J, Peterson AM, Jiang Q, Wang JQ, Chu X-P. Acid-sensing ion channels and mechanosensation. *Int J Mol Sci*. 2021;22(9):4810. doi:10.3390/ijms22094810

21. Malko P, Jiang LH. TRPM2 channel-mediated cell death: an important mechanism linking oxidative stress-inducing pathological factors to associated pathological conditions. *Redox Biol*. 2020;37:101755. doi:10.1016/j.redox.2020.101755

22. Zhang W, Chen Y, Qin J, et al. Prolonged sevoflurane exposure causes abnormal synapse development and dysregulates beta-neurexin and neuroligins in the hippocampus in neonatal rats. *J Affect Disord*. 2022;312:22–29. doi:10.1016/j.jad.2022.05.115

23. Sun M, Xie Z, Zhang J, Leng Y. Mechanistic insight into sevoflurane-associated developmental neurotoxicity. *Cell Biol Toxicol*. 2022;38 (6):927–943. doi:10.1007/s10565-021-09677-y

24. Liddelow SA, Barres BA. Reactive astrocytes: production, function, and therapeutic potential. *Immunity*. 2017;46(6):957–967. doi:10.1016/j.immuni.2017.06.006

25. Cenalmor A, Pascual E, Gil-Manso S, Correa-Rocha R, Suarez JR, Garcia-Alvarez I. Evaluation of anti-neuroinflammatory activity of isatin derivatives in activated microglia. *Molecules*. 2023;28(12):4882. doi:10.3390/molecules28124882

26. Medvedev A, Kopylov A, Buneeva O, et al. A neuroprotective dose of isatin causes multilevel changes involving the brain proteome: prospects for further research. *Int J Mol Sci*. 2020;21(11):4187. doi:10.3390/ijms21114187

27. Liddelow SA, Guttenplan KA, Clarke LE, et al. Neurotoxic reactive astrocytes are induced by activated microglia. *Nature*. 2017;541 (7638):481–487. doi:10.1038/nature21029

28. Feng X, Valdearcos M, Uchida Y, Lutrin D, Maze M, Koliwad SK. Microglia mediate postoperative hippocampal inflammation and cognitive decline in mice. *JCI Insight*. 2017;2(7):e91229. doi:10.1172/jci.insight.91229

29. Guo S, Liu L, Wang C, Jiang Q, Dong Y, Tian Y. Repeated exposure to sevoflurane impairs the learning and memory of older male rats. *Life Sci*. 2018;192:75–83. doi:10.1016/j.lfs.2017.11.025

30. Heppner FL, Ransohoff RM, Becher B. Immune attack: the role of inflammation in Alzheimer disease. *Nat Rev Neurosci*. 2015;16(6):358–372. doi:10.1038/nrn3880

31. Saijo K, Glass CK. Microglial cell origin and phenotypes in health and disease. *Nat Rev Immunol*. 2011;11(11):775–787. doi:10.1038/nri3086

32. Tang BL. Glucose, glycolysis, and neurodegenerative diseases. *J Cell Physiol*. 2020;235(11):7653–7662. doi:10.1002/jcp.29682

33. Wang YM, Liu HX, Fang NY. High glucose concentration impairs 5-PAHSA activity by inhibiting AMP-activated protein kinase activation and promoting nuclear factor-kappa-B-mediated inflammation. *Front Pharmacol*. 2018;9:1491. doi:10.3389/fphar.2018.01491

34. Ammini CV, Fernandez-Canon J, Shroads AL, et al. Pharmacologic or genetic ablation of maleylacetoacetate isomerase increases levels of toxic tyrosine catabolites in rodents. *Biochem Pharmacol*. 2003;66(10):2029–2038. doi:10.1016/j.bcp.2003.07.002

35. Burlina A, Giuliani A, Polo G, et al. Detection of 3-O-methyldopa in dried blood spots for neonatal diagnosis of aromatic L-amino-acid decarboxylase deficiency: the northeastern Italian experience. *Mol Genet Metab*. 2021;133(1):56–62. doi:10.1016/j.ymgme.2021.03.009

36. Lee ES, Chen H, King J, Charlton C. The role of 3-O-methyldopa in the side effects of L-dopa. *Neurochem Res*. 2008;33(3):401–411. doi:10.1007/s11064-007-9442-6

37. Asanuma M, Miyazaki I. 3-O-Methyldopa inhibits astrocyte-mediated dopaminergic neuroprotective effects of L-DOPA. *BMC Neurosci*. 2016;17(1):52. doi:10.1186/s12868-016-0289-0

38. Zhang YZ, Du HZ, Liu HL, He QS, Xu Z. Isatin dimers and their biological activities. *Arch Pharm*. 2020;353(3):e1900299. doi:10.1002/ardp.201900299

39. Medvedev A, Igosheva N, Crumeyrolle-Arias M, Glover V. Isatin: role in stress and anxiety. *Stress*. 2005;8(3):175–183. doi:10.1080/10253890500342321

40. Brandao P, Marques C, Burke AJ, Pineiro M. The application of isatin-based multicomponent-reactions in the quest for new bioactive and druglike molecules. *Eur J Med Chem*. 2021;211:113102. doi:10.1016/j.ejmech.2020.113102